Strongly correlated systems in atomic and condensed matter physics

Lecture notes by Eugene Demler

ETH

November 1, 2023

Chapter 8

Quantum noise measurements as a probe of many-body states

8.1 Quantum Noise

Analysis of noise is a useful tool in many areas of physics. One famous example is Haburry-Brown-Twiss effect used in astronomy. Consider two incoherent distant sources, such as two ends of a star. One can not use a single detector to observe interference between the sources. When sources are incoherent, a single detector always measures the sum of the two intensities. However Haburry-Brown and Twiss realized that one can use two detectors to measure correlations of the intensities[2, 3]. This correlation function now contains an oscillating terms that depends on the relative angle of the light rays arriving from the two sources (see fig.15.1). HBT correlations are now commonly used to measure angular diameter of stars[8].

Another canonical example of noise is shot noise in electron transport. Consider electric current going through some material, say a simple electrical wire. We can choose a certain cross section of the wire and measure charge going through during time τ. We do such measurements several times and compare the results. On the average (i.e. averaged over many runs) this charge is $\langle Q \rangle = \langle I \rangle \tau$. But there will also be shot to shot fluctuations. At sufficiently low temperatures shot noise due to discreetness of electron charge will dominate over thermal noise and fluctuations will be given by $\langle (Q - \langle Q \rangle)^2 \rangle = 2eI\tau$. W. Shottky suggested this as a way of measuring electron charge back in 1918 [11]. Currently this technique is used to explore exotic electronic states, such as fractional quantum Hall states. Noise measurements provided one of the strongest evidence for the Laughlin picture of the fractional quantum Hall state by demonstrating that the quasiparticle charge at $\nu = 1/3$ was precisely $e/3$[9].

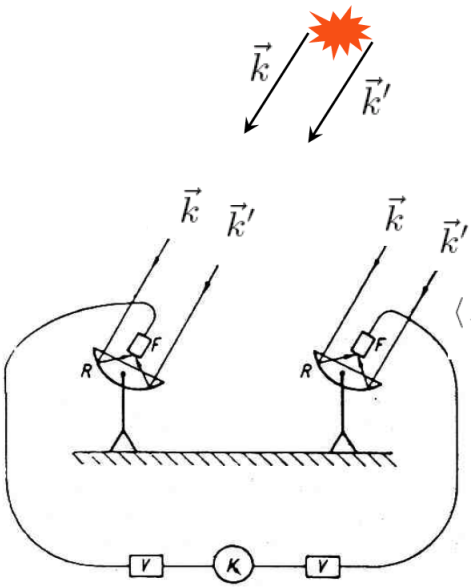

Figure 8.1: HBT measurements of the angular distance between two incoherent sources. Correlation function of the intensities contains oscillaltions which depend on the angle between incoming light rays. $\langle I_1\, I_2 \rangle = A + B\cos(\,(\vec{k} - \vec{k}')\,(\vec{r}_1 - \vec{r}_2)\,)$

In this chapter we will discuss how one can use analysis of noise to study many-body systems of ultracold atoms. Our focus will be on the quantum noise measurements in the TOF experiments. Quantum noise is one of the most fundamental concepts in quantum mechanics. Any quantum mechanical system is described by a wavefunction, and doing a measurement on a quantum system collapses this wavefunction. The wavefunction can be used to predict probabilities of different measurements, but results of individual measurements will not generically coincide with the average value (i.e. results of the measurement averaged over many experimental runs). This difference between a single shot measurement and the average value is called quantum noise. It reflects intrinsically probabilistic character of quantum mechanics. Quantum noise depends on the state of the system, so by analyzing this noise we expect to learn something about the system. While this is obvious for simple quantum systems, such as the one shown in figure 15.2, we will see that this argument can also be used for strongly correlated many-body systems.

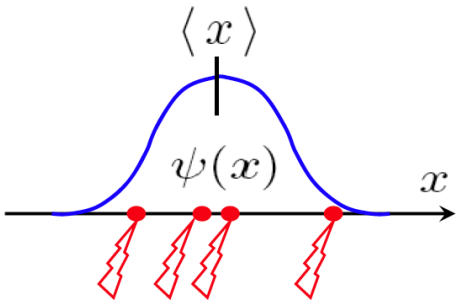

Figure 8.2: Illustration for the idea of quantum noise. A particle is described by a 1d Schroedinger wavefunction. When position of the particle is measured, this wavefunction is collapsed to a state with a certain position. The wavefunction can be used to predict probaiblities to find the particle at different points. The average position is defined as a result of many measurements. Result of an individual measurement does not generically coincide with what one finds after averaging over many shots. The difference between the single shot result and the average value is called quantum noise.

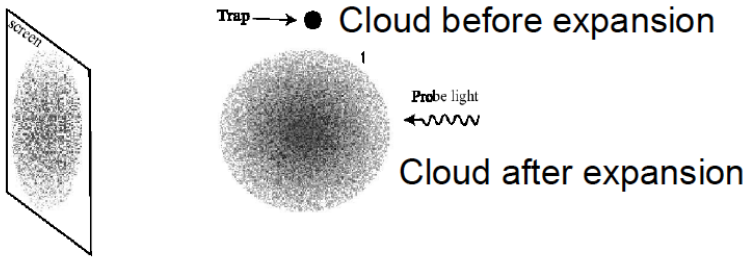

Figure 8.3: Schematic picture of TOF experiments (courtesy of E. Altman).

8.2 Second order correlations in TOF experiments

Our goal is to understand what information can be extracted from the time-of-flight (TOF) experiments. A brief reminder: TOF experiments correspond to suddenly switching off the confining potential (and the optical lattice potential if present) and letting an atomic ensemble expand. When the cloud expands to a size which is much larger than its original size, it is imaged by shining a laser beam (see fig. 15.3). During the expansion the density drops so rapidly that the probability of atomic collisions quickly becomes negligible. In many cases it is reasonable to assume that during the TOF expansion atoms propagate ballistically. In our discussion in this section we assume that the probability of an atom

to undergo a collision integrated over the entire expansion process is negligible. Then we have a situation when atoms start expanding with velocities that they had inside the many-body system and then continue to propagate with precisely the same velocities. Such assumption is particularly well justified for systems confined in optical lattices. In this case atoms have a lot of kinetic energy due to initial strong confinement within individual wells. Even for systems close to Feshbach resonances (where interactions are strong) ballistic expansion can be achieved by turning off the scattering length right during the expansion using magnetic field.

Previously we said that TOF experiments map momentum distribution into real space images. Here is a more precise statement: the density of particles at point r after the expansion time t is given by the occupation number of particles in momentum space before the expansion

$$\langle \rho_\sigma(r,t)\rangle \propto = \left(\frac{m}{\hbar\, t}\right)^3 \langle n_{k\sigma}(t=0)\rangle \equiv \left(\frac{m}{\hbar\, t}\right)^3 \langle b^\dagger_{k\sigma} b_{k\sigma}\rangle (t=0) \quad (8.1)$$

$$k(r) = \frac{mr}{\hbar t} \quad (8.2)$$

These equations assume that expansion of particles is fully ballistic, i.e. there are no collisions during the expansion time t. We can obtain (15.1), (15.2) by considering the time evolution of the operator $\Psi^\dagger_\sigma(r)$ in the Heisenberg representation

$$\Psi^\dagger_\sigma(r,t) = \int d^3k\; b^\dagger_{k\sigma}(t)\, e^{ikr} = \int d^3k\, b^\dagger_{k\sigma}(0)\, e^{i\,(\,kr\,-\,\frac{\hbar^2 k^2 t}{2m}\,)}$$

$$= \int d^3k\, b^\dagger_{k\sigma}(0)\, e^{-i\,\frac{\hbar t}{2m}(\vec{k}-\frac{m\vec{r}}{\hbar t})^2 \,+\, i\frac{mr^2}{2\hbar t}} \quad (8.3)$$

When the expansion time is sufficiently long, we can use the steepest descent method of integration and find

$$\Psi^\dagger_\sigma(r,t) = \left(\frac{m}{\hbar\, t}\right)^{3/2} b^\dagger_{k(r)\sigma}\, e^{i\,\frac{\hbar^2 k^2(r) t}{2m}} \quad (8.4)$$

From the last equation and the definition of the density operator $\rho_\sigma(r,t) = \Psi^\dagger_\sigma(r,t)\,\Psi_\sigma(r,t)$ we obtain equations (15.1), (15.2).

In this chapter we will discuss what information can be extracted from TOF images beyond $\langle b^\dagger_{k\sigma} b_{k\sigma}\rangle$. Our focus will be on analyzing second order correlation functions

$$g_{2\sigma\sigma'}(r,r') \;=\; \langle\, \delta\rho_\sigma(r)\, \delta\rho_{\sigma'}(r')\,\rangle \quad (8.5)$$

where

$$\delta\rho_\sigma(r) = \rho_\sigma(r,t) - \langle\, \rho_\sigma(r,t)\rangle \quad (8.6)$$

and $\langle \dots \rangle$ means averaging over many shots. g_2 measures correlations in fluctuations of the particle number (after TOF expansion). This correlation function

goes beyond analyzing the average number of particles at point r to ask about the probability to find particles at point r', when we know the number of particles detected at point r. For example, if a certain shot shows extra particles at point r (relative to the average number), g_2 tells us whether we should expect a positive or a negative fluctuation in the number of particles at point r' (relative to the average number) in the same shot. Figures 15.4 and 15.8 show examples of TOF images. You can see that each of them contains a noisy part on top of the overall smooth structure. It is this noise that we plan to analyze in this section.

Let us start be relating (15.5) to some correlation function before the expansion

$$\begin{aligned} \langle \rho_\sigma(r)\, \rho_{\sigma'}(r') \rangle &= \langle \Psi^\dagger_\sigma(r,t)\, \Psi_\sigma(r,t)\, \Psi^\dagger_{\sigma'}(r',t)\, \Psi_{\sigma'}(r',t) \rangle \\ = \delta(r-r')\delta_{\sigma\sigma'} \langle \rho_\sigma(r,t) \rangle &\pm \langle \Psi^\dagger_\sigma(r,t)\, \Psi^\dagger_{\sigma'}(r',t)\, \Psi_\sigma(r,t)\, \Psi_{\sigma'}(r',t) \rangle \end{aligned} \quad (8.7)$$

In the last equation we have $+$ sign for bosons and $-$ sign or fermions. The first term in (15.7) arises from measuring the same particle twice. For the long TOF expansion we apply relation (15.4) to write

$$\langle : \rho_\sigma(r)\, \rho_{\sigma'}(r') : \rangle = \pm \left(\frac{m}{\hbar t}\right)^6 \langle b^\dagger_{k(r)\sigma}\, b^\dagger_{k'(r')\sigma'}\, b_{k(r)\sigma}\, b_{k'(r')\sigma'} \rangle \quad (8.8)$$

We added $\langle : \quad : \rangle$ in the last expression to indicate that we are taking the normal ordered expression without the $\delta(r-r')$ part.

In equation (15.8) $b^\dagger_k$ and $b^\dagger_{k'}$ are creation operators for particles with well defined physical momenta. So k and k' can take arbitrary values. On the other hand, when we discuss lattice systems it is convenient to work with creation and annihilation operators of particles in the lowest Bloch band. Generically we have $b^\dagger_k = \sum_n \alpha_{nk} b^\dagger_{n\tilde{k}}$, where n is a band index and $\tilde{k}$ is obtained from k by folding it into the Brillouin zone. We assume that before the expansion (i.e. when the optical lattice potential was still present) all atoms were in the lowest Bloch bands. Thus in our discussion we only need to keep the $n=0$ contribution. For a system of size $L\times L\times L$ we should also remember that $\tilde{k}$ should be quantized with discretization step $\Delta k_i = 2\pi/L$. However it is more convenient for us to think of $\tilde{k}$ as a continuous variable over which we can integrate. This requires introducing a phase space volume factor. Thus we have

$$b^\dagger_k = \left(\frac{L}{2\pi}\right)^{3/2} \alpha_k\, b^\dagger_{\mathrm{lat}\,\tilde{k}} \quad (8.9)$$

Operators $b^\dagger_{\mathrm{lat}\,\tilde{k}}$ are eigenstates of the optical lattice potential in the lowest Bloch band. Many-body lattice Hamiltonians, such as the Hubbard model, are written in terms of these operators . Coefficients α_k are determined by wavefunctions within individual wells (see Appendix 15.7 for more details). They define how many plane-wave states are strongly mixed in a state with a given quasimomentum. When we have n_{BZ} for each direction, we can use normalization condition

to estimate $|\alpha_k|^2 \sim 1/n_{BZ}^3$ (this is a crude estimate which will suffice for our purposes. We will not need precise values of α_k).

For example, for the cloud density after the expansion we can write

$$\langle\, \rho(r)\,\rangle = \left(\frac{L}{2\pi}\right)^3 \left(\frac{m}{\hbar t}\right)^3 |\alpha_k|^2\, \langle b^\dagger_{\mathrm{lat}\,\tilde{k}}\, b_{\mathrm{lat}\,\tilde{k}}\,\rangle \tag{8.10}$$

We define

$$l = \frac{ht}{ma} \tag{8.11}$$

A particle with the velocity set by the reciprocal lattice vector, $v = h/ma$, expands during the time t by l. Then

$$\langle\rho(r)\rangle = \frac{N_{sites}}{l^3}\, |\alpha_k|^2\, \langle b^\dagger_{\mathrm{lat}\,\tilde{k}}\, b_{\mathrm{lat}\,\tilde{k}}\,\rangle \tag{8.12}$$

In a Mott state with $n = 1$ we have $\langle b^\dagger_{\mathrm{lat}\,\tilde{k}}\, b_{\mathrm{lat}\,\tilde{k}}\,\rangle = 1$ which gives $\rho(r) \approx N_{sites}/(n_{BZ}l)^3$. This is an expected result. The cloud size after the expansion is approximately $n_{BZ}l$ in each direction. So we find that the density as the total number of atoms divided by the total size of the expanded cloud. This is a crude estimate since the density is not uniform after the expansion. However it shows us that our normalization factors make sense. It will also be useful later when we estimate the magnitude of the noise signal.

We can write for equation (15.8)

$$\langle b^\dagger_k b^\dagger_{k'} b_k b_{k'}\rangle_{\mathrm{phys}} = |\alpha_k|^2\, |\alpha_{k'}|^2 \left(\frac{L}{2\pi}\right)^6 \langle b^\dagger_{\tilde{k}} b^\dagger_{\tilde{k}'} b_{\tilde{k}} b_{\tilde{k}'}\rangle_{\mathrm{lat}} \tag{8.13}$$

8.3 Mott state with $n = 1$

8.3.1 Boson bunching

We have

$$\langle b^\dagger_{\tilde{k}} b^\dagger_{\tilde{k}'} b_{\tilde{k}} b_{\tilde{k}'}\rangle_{\mathrm{lat}} \;=\; \frac{1}{N^2_{\mathrm{sites}}} \sum_{lmn\rho} \langle b^\dagger_l b^\dagger_m b_n b_\rho\rangle\, e^{-i\tilde{k}r_l} e^{-i\tilde{k}'r_m} e^{i\tilde{k}r_n} e^{i\tilde{k}'r_\rho} \tag{8.14}$$

In a Mott state we have local correlations only and

$$\langle b^\dagger_l b^\dagger_m b_n b_\rho\rangle = \delta_{ln}\delta_{m\rho} + \delta_{l\rho}\delta_{mn} \tag{8.15}$$

Then

$$\begin{aligned}\langle b^\dagger_{\tilde{k}} b^\dagger_{\tilde{k}'} b_{\tilde{k}} b_{\tilde{k}'}\rangle_{\mathrm{lat}} \;&=\; \frac{1}{N^2_{\mathrm{sites}}} \sum_{lmn\rho} (\,\delta_{ln}\delta_{m\rho} + \delta_{l\rho}\delta_{mn}\,)\, e^{-i\tilde{k}r_l} e^{-i\tilde{k}'r_m} e^{i\tilde{k}r_n} e^{i\tilde{k}'r_\rho} \\ &=\; \frac{1}{N^2_{\mathrm{sites}}} \sum_{ln} 1 + \frac{1}{N^2_{\mathrm{sites}}} \sum_{ln} e^{i(\tilde{k}-\tilde{k}')(r_n - r_l)}\end{aligned} \tag{8.16}$$

We should be careful when doing lattice summation since we have a finite number of sites in the lattice. We have

$$\frac{1}{N_{sites}^2}\sum_{ln} e^{iq(r_n-r_l)} = \frac{\sin^2(N_x q_x a/2)}{\sin^2(q_x a/2)}\frac{\sin^2(N_y q_y a/2)}{\sin^2(q_y a/2)}\frac{\sin^2(N_z q_z a/2)}{\sin^2(q_z a/2)} \tag{8.17}$$

We get peaks of height 1 (use $N_x N_y N_z = N_{sites}$) and width $\Delta q_x = 2\pi/aN_x = 2\pi/L$. Hence we can write

$$\frac{1}{N_{sites}^2}\sum_{ln} e^{iq(r_n-r_l)} = \left(\frac{2\pi}{L}\right)^3 \sum_G \delta(q-G) \tag{8.18}$$

Here G are reciprocal lattice vectors of the optical lattice. We can also consider the last equation as taking a continuum limit of the discreet delta-function for lattice wavevectors.

We have

$$\langle : \rho_\sigma(r)\,\rho_{\sigma'}(r') : \rangle = \left(\frac{L}{2\pi}\right)^6 \left(\frac{m}{\hbar t}\right)^6 |\alpha_k|^2\,|\alpha_{k'}|^2(1+\left(\frac{2\pi}{L}\right)^3 \delta(k-k'-G)) \tag{8.19}$$

where $k(r)$ and $k'(r')$ are given by equation (15.2). Combining this result with equation (15.12) for $\langle b^\dagger_{\text{lat}\,\tilde{k}}\, b_{\text{lat}\,\tilde{k}}\rangle$ (we have a Mott state with $n = 1$) and recalling that $\tilde{k}$ differs from k by reciprocal lattice vectors G we find

$$\langle : \delta\rho(r)\,\delta\rho(r') : \rangle = (\frac{m}{\hbar t})^6 \left(\frac{L}{2\pi}\right)^3 |\alpha_{k(r)}|^2\,|\alpha_{k'(r)}|^2 \sum_G \delta(k(r)-k'(r')-G) \tag{8.20}$$

We can now use $\delta(k) = (\frac{a}{2\pi})^3\delta(k\cdot\frac{a}{2\pi})$ and $\frac{ma}{2\pi\hbar t} = \frac{1}{l}$ to write

$$\begin{aligned}\langle : \delta\rho(r)\,\delta\rho(r') : \rangle &= (\frac{m}{\hbar t})^6 \left(\frac{L}{2\pi}\right)^3 |\alpha_{k(r)}|^2\,|\alpha_{k'(r)}|^2\,(\frac{a}{2\pi})^3 \sum_{p_n}\delta(\frac{\vec{r}-\vec{r}'}{l}-\vec{p}_n)\\ &= \frac{N_{sites}}{l^6}\,|\alpha_{k(r)}|^2\,|\alpha_{k'(r)}|^2 \sum_{p_n}\delta(\frac{r-r'}{l}-p_n)\end{aligned} \tag{8.21}$$

Here $\vec{p}_n = \frac{a\,\vec{G}}{2\pi}$. For a simple cubic lattice we have $\vec{p}_n$ of the form $\{(1,0,0),(0,1,0),(0,0,1),(1,1,0),...,(2,0,0),...\}$.

We get bunching when $k-k'$ corresponds to the reciprocal lattice of the optical lattice. A simple physical interpretation of this result in terms of the Hanburry-Brown-Twiss Boson bunching is presented in section 15.3.3. Experimental measurements of boson correlations in TOF experiments from the Mott state are shown in fig. 15.4.

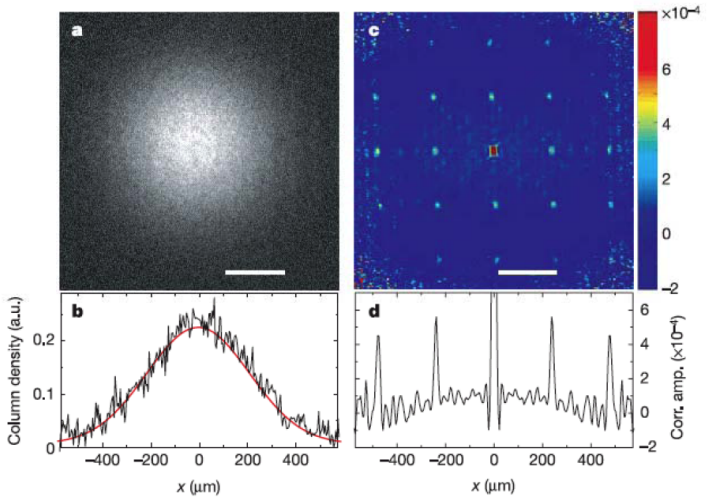

Figure 8.4: Bosonic bunching in the TOF experiments from the Mott state of bosons. Figures taken from [5].

8.3.2 Order of magnitude Estimate

To understand the magnitude of the effect in real experiments we need to deal with the issue of integrating over the imaging axis. When we take correlation functions over two dimensional images we have

$$g_{2\,2dim}(r_\perp, r'_\perp) = \int dz\, dz'\, g_2(r, r') \tag{8.22}$$

Integration over z and z' picks up contributions which differ in $z - z' = n\,l$. Each of these delta functions contributes l the number of such contributions is n_{BZ}. Hence the total of z and z' integration is $(l n_{BZ})^2$. Thus we find

$$g_{2\,2dim} = \frac{N_{sites}}{(l n_{BZ})^6}\,(l n_{BZ})^2 \sum_{p_n} \delta^{2d}\left(\frac{r - r'}{l} - p_n\right) \tag{8.23}$$

In experiments it is also more convenient to define

$$C_2 = \frac{g_{2\,2dim}(r_\perp, r'_\perp)}{\langle \rho_{2dim}(r_\perp)\rangle \,\langle \rho_{2dim}(r'_\perp)\rangle} \tag{8.24}$$

Integration over z gives $\langle \rho_{2dim}(r_\perp)\rangle \approx \rho_{3dim} l n_{BZ} \approx N_{sites}/(l n_{BZ})^2$. Hence

$$C_2 = \frac{1}{N_{sites}} \sum_{p_n} \delta^{2d}\left(\frac{\vec{r}_\perp - \vec{r}'_\perp}{l} - \vec{p}_{n\perp}\right) \tag{8.25}$$

To include finite detector resolution we replace

$$\delta^{2dim}\left(\frac{\vec{d}}{l}\right) = \frac{1}{4\pi}\left(\frac{l}{\sigma}\right)^2 e^{-d^2/4\sigma^2} \tag{8.26}$$

Then

$$C_2 = \frac{1}{4\pi N_{sites}} \left(\frac{l}{\sigma}\right)^2 \sum_{p_n} e^{-(\vec{d}-\frac{t}{m}\vec{p}_n)^2/4\sigma^2} \tag{8.27}$$

In typical experiments $l/\sigma \approx 40$ and $N_{sites} \approx 5 \times 10^5$. Thus the signal in $C(d)$ is about 3×10^{-4}. This number agrees with the experimental results shown in fig. 15.4.

8.3.3 Semiclassical picture. Interference of independent condensates

Our derivation of the boson bunching in (15.21) was based on the fully quantum description. In the case of bosons we can also give a classical interpretation of this phenomenon.

Let us start with a conceptually simpler problem of interference of two independent condensates. Such experiments have been among the first experiments done with BECs of ultracold atoms[4]. Consider a setup shown in figure 15.5. Two condensates are prepared in traps 1 and 2. At time $t = 0$ atoms are released, the clouds expand, and the density is measured at point r. We can schematically write for the wavefunction at point r and time t

$$\Psi(r,t) \sim e^{i\phi_1} e^{i\frac{m(\vec{r}+\vec{d})^2}{\hbar t}} + e^{i\phi_2} e^{i\frac{m(\vec{r})^2}{\hbar t}} \tag{8.28}$$

Here ϕ_1 and ϕ_2 are phases of the original condensates before the expansion. Then the density has an interference term

$$\rho_{\rm int}(r) = e^{i(\phi_1-\phi_2)+i\frac{m\vec{r}\vec{d}}{\hbar t}} \tag{8.29}$$

When two condensates are not correlated $\langle e^{i(\phi_1-\phi_2)}\rangle = 0$. However this does not mean that we do not have interference pattern. It simply means that after averaging over many shots interference pattern will disappear. A single shot can still show a perfect interference pattern (see fig. 15.6). Let us consider two point correlation function

$$\langle \rho_{\rm int}(r)\rho_{\rm int}(r')\rangle = e^{i\frac{m\vec{r}\vec{d}}{\hbar t}} + \text{c.c.} \tag{8.30}$$

We see periodic oscillations in the second order correlation function. This means that when we have interference of two uncorrelated condensates, we can not predict whether point r will have a maximum or a minimum of the interference pattern. However we can predict that if we find a maximum at point r it will be followed by another maximum a distance ht/md away. This is an example of the "quantum noise". Results of an individual measurement are generically different from averaging over many measurements.

Now imagine a periodic lattice of independent condensates. We can assume that each condensate has a random phase. When we let all these condensates

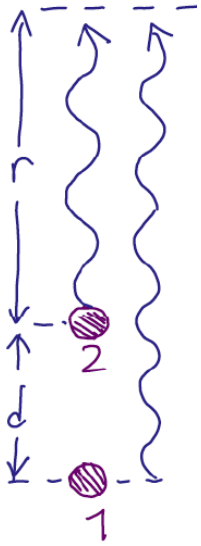

Figure 8.5: Schematic picture of interference experiments with two independent condensates.

to expand we find correlations between all possible pairs. So we can write

$$\langle\, \delta\rho(r)\, \delta\rho(r')\, \rangle \sim 2\cos(\frac{m\vec{r}}{\hbar t}\,\vec{a}_x) + 2\cos(\frac{m\vec{r}}{\hbar t}\,2\vec{a}_x) + 2\cos(\frac{m\vec{r}}{\hbar t}\,\vec{a}_y) + \cdots \quad (8.31)$$

We used $a_{\{x,y\}}$ to denote lattice constants in different directions. When we add up all terms (15.31) we find delta functions at reciprocal lattice vectors as in (15.21).

$$\langle\, \delta\rho(r)\, \delta\rho(r')\, \rangle \sim \sum_G \delta(k(r) - k'(r') - G) \quad (8.32)$$

with $\hbar k(r)t/m = r$. A "semiclassical" picture of the Mott state is precisely that: condensates with random uncorrelated phases. Interference experiments with a one dimensional array of uncorrelated condensates have been performed by Hadzibabic et al. (see fig. 15.7). The difference of experiments by Hadzibabic et al. [7] with the experiments of Foelling et al. [5] is that the former experiments have a large number of particles per well and a relatively small number of wells. As a result, individual shots appear to have interference like pattern. One can check, however, that this is still noise type correlations by repeating these experiments many times. Then one finds that interference patterns averaged over many shots disappear. By contrast, when the potential between individual wells is lowered and condensates in different wells begin to establish phase coherence with each other, interference patterns survive even after averaging over many shots (see fig. 15.7).

It is also instructive to draw analogy between bosons bunching in TOF experiments in optical lattices (see eq. (15.32)) and the optical HBT effect discussed

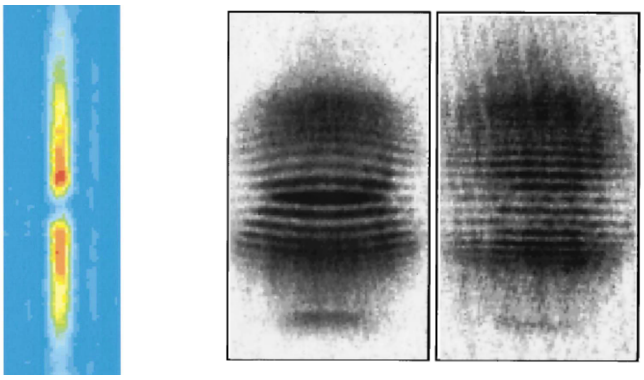

Figure 8.6: A single shot image of two independent macroscopic condensates after expansion. Figure taken from ref [4]. Individual shots show perfect interference patterns. However the phase of interference fringes is random from shot to shot. Averaging over may shots would wash out interference fringes.

in fig. 15.1. In the Mott state we do not have a macroscopic occupation of a state with a certain quasimomentum. All quasimomenta are occupied. However let us consider free expansion of atoms from just one of them. Later we will add contributions from all quasimomenta. Bosons starting from quasimomentum $\tilde{k}$ expand as a collection of plane waves which differ by reciprocal lattice vectors $k = \tilde{k} + G$. These states together produce a perfect interference pattern. Now we take another quasimomentum state $\tilde{k}'$. Bosons from this state also produce a perfect interference pattern, but it is shifted with respect to the previous one. When we add contributions from all quasimomenta, we find that interference patterns wash each other out. So in the density itself we no longer have sharp interference peaks (no first order coherence). However we realize that our system has many "particle beams" propagating at different momenta, so in the spirit of HBT we can ask about two point correlations. According to HBT we expect oscillations in $\langle : \delta\rho(r)\,\delta\rho(r') : \rangle$ determined by relative vavectors of different pairs of beams. And there is a set of relative wavevectors that repeats itself over and over. These are reciprocal lattice vectors.

8.4 Band Insulating State of Fermions

We now consider spinless fermions in an optical lattice. We assume that the system has filling factor one, so we have a band insulator.

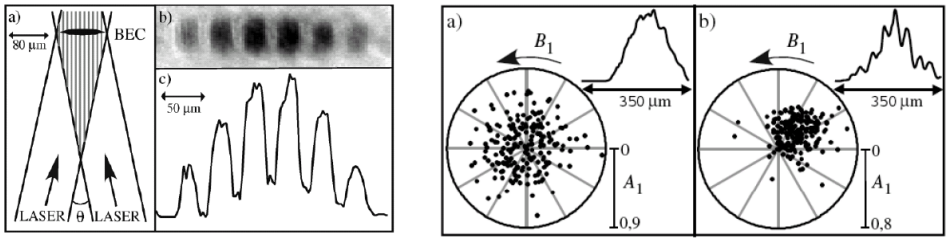

Figure 8.7: Interference patterns from a one dimensional array of condensates. Figures taken from [7]. Even when condensates are decoupled individual shots appear to have an interference pattern (figure c) on the left). However in this case the position of fringes is random from shot to shot. This is shown in figure a) on the right. The main figure shows results of many interference experiments in the representation where the amplitude and the phase of the interference fringes are represented as the radius and the angle respectively. In this case of decoupled condensates phases of interference fringes are random from shot to shot. Figure b) on the right corresponds to experiments where particles are allowed to tunnel between condensates. All interference patterns show very similar phase of the fringes.

We consider second order correlations

$$\begin{aligned}\langle \quad : \rho(r)\,\rho(r') : \rangle &= -(\frac{m}{\hbar t})^6 \left(\frac{L}{2\pi}\right)^3 |\alpha_{k(r)}|^2\,|\alpha_{k'(r)}|^2\,\langle\, f^\dagger_{k(r)}\, f^\dagger_{k'(r')}\, f_{k(r)}\, f_{k'(r')}\,\rangle \\ &= -(\frac{m}{\hbar t})^6 \left(\frac{L}{2\pi}\right)^3 |\alpha_{k(r)}|^2\,|\alpha_{k'(r)}|^2\,\frac{1}{N^2_{sites}}\sum_{lmn\rho}\langle\, f^\dagger_l\, f^\dagger_m f_n f_\rho\,\rangle, e^{-i\tilde{k}r_l} e^{-i\tilde{k}'r_m} e^{i\tilde{k}r_n} e^{i\tilde{k}'r_\rho}\end{aligned} \tag{8.33}$$

We use $f\dagger$ for creation operators to emphasize that we are analyzing fermions. In the band insulating state we have only local correlations

$$\langle\, f^\dagger_l\, f^\dagger_m f_n f_\rho\,\rangle = -\delta_{ln}\delta_{m\rho} + \delta_{l\rho}\delta_{mn} \tag{8.34}$$

Then

$$\begin{aligned}\langle : \delta\rho(r)\,\delta\rho(r') : \rangle &= -(\frac{m}{\hbar t})^6 \left(\frac{L}{2\pi}\right)^3 |\alpha_{k(r)}|^2\,|\alpha_{k'(r)}|^2 \sum_G \delta(k(r) - k'(r') - G) \\ &= -\frac{N_{sites}}{l^6}\,|\alpha_{k(r)}|^2\,|\alpha_{k'(r)}|^2 \sum_{p_n}\delta(\frac{r-r'}{l} - p_n)\end{aligned} \tag{8.35}$$

In the case of fermions we find antibunching rather than bunching. This can be understood as Pauli priniciple. A single particle state with quasimomentum $\tilde{k}$ is a superposition of states with physical momenta $\tilde{k} + G$. When we detect a fermion at momentum $\tilde{k} + G_1$, we decrease the probability to find another fermion at momentum $\tilde{k} + G_2$. Fermionic antibunching in TOF experiments measure by T. Rom et al. [6] is shown in figure 15.8.

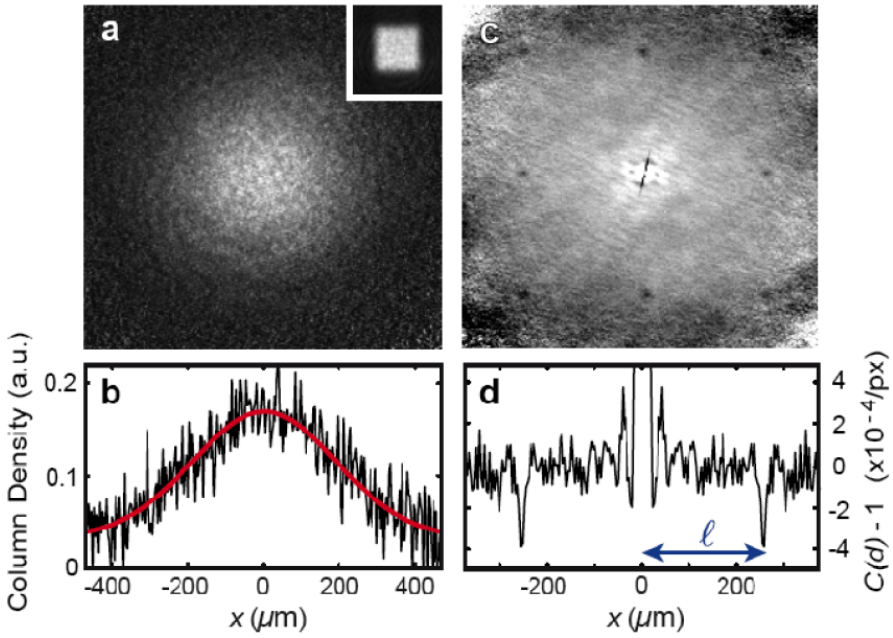

Figure 8.8: Fermionic antibunching in the TOF experiments from the band insulating state of bosons. Figures taken from [6].

8.5 Two particle interference

Both bosonic bunching discussed in section 15.3.1 and fermionic antibunching discussed in section 15.4 can be interpreted in terms of the two particle interference known as the Hanburry-Brown-Twiss effect[2, 3, 1]. This is schematically shown in figure 15.9. There are two sources and two detectors. When two particles are observed in the two detectors, we can have particle in the first detector arriving from the first source, and particle in the second detector arriving from the second source. Alternatively we can have these particles interchanged. In quantum mechanics we need to add the two amplitudes and then take the square to calculate the intensity. When the two particles are bosons, we add the amplitudes with the plus sign. When the particles are fermions, we add the amplitudes with the minus sign. The cross term of the two amplitudes gives rise to HBT correlations [10].

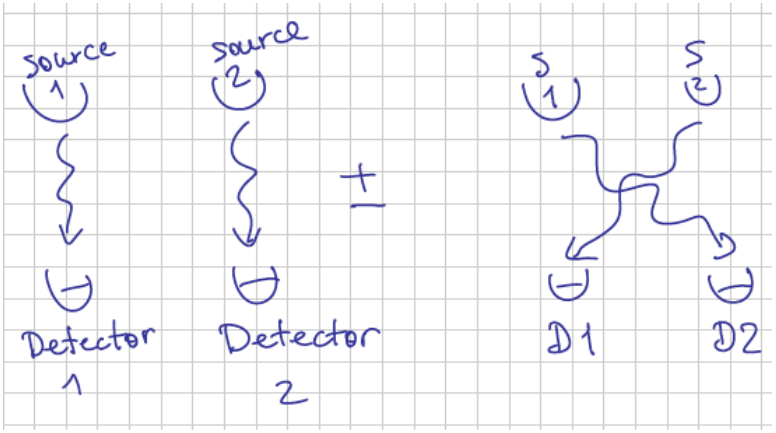

Figure 8.9: Schematic representation of two particle interference. Two amplitudes are added with the plus sign in the case of bosons. They are added with the minus sign in the case of fermions.

8.6 Bosons with spin. Mott state with AF order.

In a state with magnetic order we have a new expectation value of the non-local order parameter. For example, when we have antiferromagnetic order with components N^x, N^y, N^z we have

$$\langle S^a(r)\rangle = \langle b^\dagger_\sigma(r)\sigma^a_{\sigma\sigma'}b_{\sigma'}(r)\rangle = (-)^r N^a \tag{8.36}$$

This new expectation value changes four boson correlation functions

$$\langle\, b^\dagger_{l\sigma}b^\dagger_{m\sigma'}b_{n\sigma}b_{\rho\sigma'}\,\rangle = \delta_{ln}\delta_{m\rho} + \delta_{\sigma\sigma'}\,\delta_{l\rho}\delta_{mn} + \delta_{l\rho}\delta_{mn}\langle\vec{S}_{\sigma'\sigma}(r_n)\rangle\,\langle\vec{S}_{\sigma\sigma'}(r_l)\rangle \tag{8.37}$$

and we get a new contribution to the four particle correlator

$$\begin{aligned}
\langle b^\dagger_{\tilde{k}\sigma}b^\dagger_{\tilde{k}'\sigma'}b_{\tilde{k}\sigma}b_{\tilde{k}'\sigma'}\rangle_{\rm lat} &= \frac{1}{N^2_{\rm sites}}\sum_{lmn\rho}\langle b^\dagger_{l\sigma}b^\dagger_{m\sigma'}b_{n\sigma'}b_{\rho\sigma}\rangle\, e^{-i\tilde{k}r_l}e^{-i\tilde{k}'r_m}e^{i\tilde{k}r_n}e^{i\tilde{k}'r_\rho} \\
&= \text{old terms} + \frac{1}{N^2_{\rm sites}}\sum_{lna} N^a_{\sigma\sigma'}N^a_{\sigma'\sigma}e^{iQ(r_n-r_l)}\,e^{i(\tilde{k}-\tilde{k}')(r_n-r_l)} \\
&= \text{old terms} + \delta(\tilde{k}-\tilde{k}'-Q)
\end{aligned} \tag{8.38}$$

Here Q is the antiferromagnetic vector $(\pi/a, \pi/a, \pi/a)$. In the noise correlations of TOF images this should appear as

$$\begin{aligned}
\langle\ :\delta\rho_\sigma(r)\,\delta\rho_{\sigma'}(r'):\rangle &= \text{old terms} + \\
&(\frac{m}{\hbar t})^6\left(\frac{L}{2\pi}\right)^3 |\alpha_{k(r)}|^2\,|\alpha_{k'(r)}|^2\,N^a_{\sigma\sigma'}N^a_{\sigma'\sigma}\sum_G\delta(k(r)-k'(r')-G-Q)
\end{aligned} \tag{8.39}$$

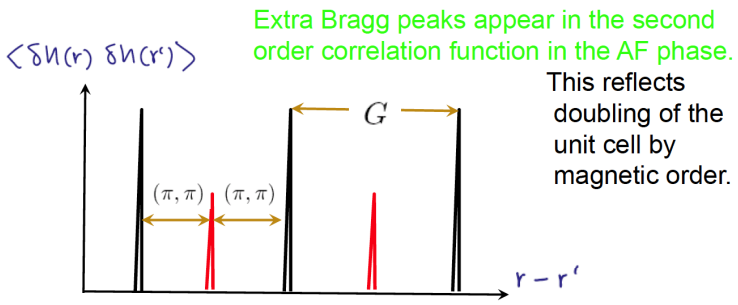

Figure 8.10: Correlation function in the Mott state of two component Bose mixture with antiferromagnetic order. AF magnetic order manifests itself in the new peaks at magnetic wavevector.

We see additional peaks at the magnetic wavevector and its Bragg reflections (see fig.15.10. Note that one does not need to do spin resolved measurements to see magnetic order in this case.

8.7 Appendix. How to calculate α_{nk}

According to the Bloch theorem single particle eigenstates of the periodic potential gan be written as (we use 1d case for simplicity)

$$\psi_{nk}(x) = e^{i\tilde{k}x} u_{n\tilde{k}}(x) \tag{8.40}$$

Function $u_{n\tilde{k}}(x)$ is peridic, i.e. $u_{n\tilde{k}}(x+a) = u_{n\tilde{k}}(x)$, where a is the period of the potential. Let us now take Fourier transform of (15.40). From periodicity of $u_{nk}(x)$ we have $u_{nk}(x) = \sum_G u_{nkG}\, e^{iGx}$, where G are reciprocal lattice vectors. Thus

$$\int dx e^{-ikx} \psi_{n\tilde{k}}(x) = \sum_G u_{n\tilde{k}G} \delta(k - \tilde{k} - G) \tag{8.41}$$

So a Bloch eigenstate with quasimomentum $\tilde{k}$ involves states with physical momentum $\tilde{k}$ (when $G = 0$) and other Bragg reflections. The number of Bragg reflections involved is determined by the Fourier transform of the function $u_{n\tilde{k}}(x)$. The latter can be thought of as the wavefunction of a particle inside an individual well. So its Fourier spectrum has a width that is inversely proportional to the size of the real space wavefunction.

8.8 Problems for Chapter 15

Problem 1

In this problem we go back to the collapse and revival experiments with (spinless) bosonic atoms in an optical lattice (M. Greiner et al. (2002)) discussed

in problem 3 in Chapter 6. Previosuly you showed that half-way between revivals the system goes through the cat state, in which $\langle b \rangle = 0$ but $\langle b^2 \rangle \neq 0$. Now you need to propose a method to detect this cat state using noise correlation analysis.

Bibliography

[1] G. Baym. *Acta Phys Pol B*, 29:1839, 1998.

[2] R.H. Brown and R.Q. Twiss. *Nature*, 177:27, 1956.

[3] R.H. Brown and R.Q. Twiss. *Nature*, 178:1447, 1956.

[4] Andrews et al. *Science*, 275:637, 1997.

[5] S. Foelling et al. *Nature*, 434:481, 2005.

[6] T. Rom et al. *Nature*, 444:733, 2006.

[7] Zoran Hadzibabic, Sabine Stock, Baptiste Battelier, Vincent Bretin, and Jean Dalibard. Interference of an array of independent bose-einstein condensates. *Phys. Rev. Lett.*, 93(18):180403, Oct 2004.

[8] HBT. *Proc. Roy. Soc. (London) A*, 248:222, 19XX.

[9] L. Saminadayar, D. C. Glattli, Y. Jin, and B. Etienne. Observation of the $e/3$ fractionally charged laughlin quasiparticle. *Phys. Rev. Lett.*, 79(13):2526–2529, Sep 1997.

[10] M. Scully and S. Zubariy. *Quantum Optics*. Cambridge Univeristy Press, 2002.

[11] W. Shottky. *Ann. Phys.*, 57:541, 1918.